remote sensing

MDPI

Article

Investigating the Role of Cover-Crop Spectra for Vineyard Monitoring from Airborne and Spaceborne Remote Sensing

Michael Williams [1,*], Niall G. Burnside [1,2], Matthew Brolly [1] and Chris B. Joyce [1]

[1] Centre for Earth Observation Science, University of Brighton, Brighton and Hove BN2 4GJ, UK; niall.burnside@sams.ac.uk (N.G.B.); m.brolly@brighton.ac.uk (M.B.); chris.joyce@jbaconsulting.com (C.B.J.)
[2] Scottish Association for Marine Sciences, Oban Argyll PA37 1QA, UK
* Correspondence: m.williams19@uni.brighton.ac.uk

Abstract: The monitoring of grape quality parameters within viticulture using airborne remote sensing is an increasingly important aspect of precision viticulture. Airborne remote sensing allows high volumes of spatial consistent data to be collected with improved efficiency over ground-based surveys. Spectral data can be used to understand the characteristics of vineyards, including the characteristics and health of the vines. Within viticultural remote sensing, the use of cover-crop spectra for monitoring is often overlooked due to the perceived noise it generates within imagery. However, within viticulture, the cover crop is a widely used and important management tool. This study uses multispectral data acquired by a high-resolution uncrewed aerial vehicle (UAV) and Sentinel-2 MSI to explore the benefit that cover-crop pixels could have for grape yield and quality monitoring. This study was undertaken across three growing seasons in the southeast of England, at a large commercial wine producer. The site was split into a number of vineyards, with sub-blocks for different vine varieties and rootstocks. Pre-harvest multispectral UAV imagery was collected across three vineyard parcels. UAV imagery was radiometrically corrected and stitched to create orthomosaics (red, green, and near-infrared) for each vineyard and survey date. Orthomosaics were segmented into pure cover-crop$_{uav}$ and pure vine$_{uav}$ pixels, removing the impact that mixed pixels could have upon analysis, with three vegetation indices (VIs) constructed from the segmented imagery. Sentinel-2 Level 2a bottom of atmosphere scenes were also acquired as close to UAV surveys as possible. In parallel, the yield and quality surveys were undertaken one to two weeks prior to harvest. Laboratory refractometry was performed to determine the grape total acid, total soluble solids, alpha amino acids, and berry weight. Extreme gradient boosting (XGBoost v2.1.1) was used to determine the ability of remote sensing data to predict the grape yield and quality parameters. Results suggested that pure cover-crop$_{uav}$ was a successful predictor of grape yield and quality parameters (range of R^2 = 0.37–0.45), with model evaluation results comparable to pure vine$_{uav}$ and Sentinel-2 models. The analysis also showed that, whilst the structural similarity between the both UAV and Sentinel-2 data was high, the cover crop is the most influential spectral component within the Sentinel-2 data. This research presents novel evidence for the ability of cover-crop$_{uav}$ to predict grape yield and quality. Moreover, this finding then provides a mechanism which explains the success of the Sentinel-2 modelling of grape yield and quality. For growers and wine producers, creating grape yield and quality prediction models through moderate-resolution satellite imagery would be a significant innovation. Proving more cost-effective than UAV monitoring for large vineyards, such methodologies could also act to bring substantial cost savings to vineyard management.

Keywords: precision agriculture; UAV; satellite; remote sensing; cover crop; quality; yield

Citation: Williams, M.; Burnside, N.G.; Brolly, M.; Joyce, C.B. Investigating the Role of Cover-Crop Spectra for Vineyard Monitoring from Airborne and Spaceborne Remote Sensing. *Remote Sens.* **2024**, *16*, 3942. https://doi.org/10.3390/rs16213942

Academic Editor: Frédéric Cointault

Received: 30 August 2024
Revised: 10 October 2024
Accepted: 19 October 2024
Published: 23 October 2024

1. Introduction

Precision Viticulture

Within viticulture, the management of grape yield and quality variation is vital for the performance of business. The effective management of the vineyard will control the vine

environment to ensure the desired level of ripening for the grape and therefore the desired qualities in the wine. Factors such as the availability of nutrients and water, temperatures, sunlight exposure, pests and disease all have important effects on grape variability. Over many centuries, management practices have developed to help control these factors and ensure the quality of the produced grapes and wine.

A key element of both historical and modern viticulture is applying management methodologies in response to data characterising vine variance. This guided approach to vine management ensures the correct level of management for grapes to reach the desired quality parameters. Historically, monitoring a vineyard has required a person walking the vines, using human intuition to observe and record important information. However, the increasing integration of technology in the industry has developed new monitoring methodologies. One of the key technologies emerging within precision viticulture is the use of airborne remote sensing to generate data and characterise changes. Satellite Earth observation (EO) and uncrewed aerial vehicles (UAVs) produce spatially continuous data with significantly higher efficiency than ground-based monitoring. The use of a broad spectral range can also help identify variation and disease, which would otherwise be missed by the human eye [1]. One of the most impactful applications of remote sensing is the monitoring or prediction of grape yield and quality parameters. Understanding the expected grape yield and quality variation prior to harvest would allow management strategies to be modified to achieve the desired quality parameters or support selective harvesting.

Research has shown that grape yield and quality, the physiological appearance of the vines, and the spectral characteristics of the vine can be associated [2]. This three-way interaction then allows a proxy relationship to be made between grape yield and quality and the spectral data observed by multispectral remote sensing. With the continuing development of both UAV and satellite remote sensing, an important discussion is which remote sensing platform is best suited to vineyard monitoring. Due to their different operating heights (UAV typically 30–100 m, satellite EO typically 150–600 km), the two platforms offer largely different spatial resolutions and costs. UAVs provide low-cost, high-resolution solutions (<0.10 m spatial resolution) whilst satellites provide low-cost, moderate-resolution solutions (>10 m spatial resolution). Whilst very-high-resolution (VHR) satellite imagery exists (<1 m), this typically has a price point which is significantly higher than UAV solutions for local studies. Therefore, the required spatial resolution for monitoring is a key factor in the decision between UAV or satellite monitoring.

The critical difference between UAV and moderate-resolution satellite monitoring is the UAVs' ability to create pure vine pixels. This is possible due to the pixel size (e.g., 0.10 m) being lower than the width of the vine row (typically 0.75–1.00 m). A pixel size larger than 1.00 m would result in mixed-feature pixels containing both vine and the inter-row space and cover crop. The impact of spatial resolution and mixed-feature pixels has been commented on in previous research. Zarco-Tejeda et al. [3] deployed aircraft hyperspectral remote sensing to assess vineyard condition. Alongside recommendations for future works, Zarco-Tejeda et al. [3] stated the importance of achieving <1.0 m spatial resolution to focus their analysis on the vines whilst masking out the inter-row space. Matese et al. [4] also suggested that lower-resolution satellite pixels were likely biased due to the averaging of vines and inter-row space within a pixel. Khaliq et al. [5] further stated that a lower-biomass cover-crop species produced a biased description of the vine characteristics. These studies suggest that the inclusion of inter-row space and cover crop within mixed-feature pixels hinders the ability of airborne remote sensing to monitor the vines. Therefore, this places importance upon high-resolution imagery and incentivises the use of UAVs for monitoring.

The underlying objective of the studies by Zarco-Tejeda et al. [3], Matese et al. [4], and Kasimiti et al. [6] is to focus on the monitoring of vines. This is perhaps with the assumption that the vine contains the most useful spectral information, whilst the inter-row and cover crop mostly contain noise. Interestingly, the suggested focus on vines is challenged in yield and quality monitoring, where established viticultural science highlights the importance of the inter-row for the management of grape quality parameters. Management approaches

such as mowing alternate rows, cover-crop species composition, and cover-crop biomass all have important implications for wider vineyard management and the management of grape quality variability [7,8]. If management approaches result in the spectral variation of cover crop, it presents a mechanism through which cover-crop spectra could be linked to yield and quality.

Whilst previous research has evidenced inter-row space and cover-crop spectra as noise when attempting to monitor the vine characteristics, this narrative might not apply to yield and quality monitoring due to the known importance of the cover crop within vineyard management. To date, viticultural literature has provided limited evidence on the possible direct effect of cover crop upon yield and quality; however, no evidence exists for the link between cover-crop spectra and yield and quality. If a cover crop can be shown to contain useful spectra for monitoring yield and quality, this also suggests that mixed-feature pixels, such as those acquired by a moderate-resolution satellite, could have a greater value than currently described.

This study will assess the potential of cover-crop spectra to be used within yield and quality monitoring, before investigating the influence that a cover crop has within moderate-resolution satellite imagery, and the potential implications this has for grape yield and quality monitoring.

2. Methodologies

2.1. Study Site and Sampling Design

This study was undertaken at Gusbourne Vineyard (Kent, UK), a world-renowned producer of English wine. As a northern hemisphere, cool-climate vineyard, the growing season temperatures typically average 17 °C with high precipitation throughout the year. The growing season begins with bud-burst in spring, with veraison occurring in late August, and harvest in late September or early October. During this period, the vine canopies gradually increase in biomass until leaf fall in autumn.

The site is non-contiguous, split across multiple fields of varying topography, soil types, and microclimates. Variation in the management of inter-row space and vine canopy exists across the site. Data collection targeted three fields of an identical vine clone and rootstock, with planted areas varying between 1.00 and 2.50 ha. Vine rows are 100–200 m long with 2.50 m row vine spacing and 1.50 m inter-row width. The inter-row area presents a mixture of grassland cover-crop species including Yorkshire fog grass (*Holcus lanatus*), Cowslip (*Primula veris*), and Cocksfoot grass (*Dactylis glomerate*). The cover crop presents at 10–20 cm height, depending on the mowing frequency, with the under vine areas undergoing tillage to control competition with the vine. Vineyard management requires the trimming of the vine canopy typically four times per growing season and the mowing of the inter-row space typically two to three times per growing season. Moreover, at certain locations, the inter-row space is mown on alternate rows to control the soil moisture and the resources available to the vine. The sample fields are detailed in Figure 1.

Sampling was conducted in accordance with the common viticultural practice of using individual trellis blocks as sample areas [9]. Trellis blocks are the supporting structures on which vines grow, and within the sampled vineyards, five vines were planted to each trellis; therefore, there were ten vines in each sampled block (two rows of five vines). As detailed in Figure 2, sample locations for each year are shown spatially. Samples consist of grape quality data from 100 grapes per trellis block, and UAV and Sentinel-2 imagery for these locations. In total, 165 grape samples were collected during a three-year period (2020 n = 39, 2021 n = 72, 2022 n = 54). The variance in sample size between the sample years is the result of varying resource's availability for grape collection and processing.

Figure 1. (Subfigures (**A**): top left, (**B**): right, (**C**): bottom left): Three sample vineyards, (**A**): 62 vine rows, study area of 20,000 m^2; (**B**): 8 vine rows, centre coordinates 51.047926, 0.789715, study area of 10,000 m^2; (**C**): 25 vine rows, centre coordinates, study area of 15,400 m^2.

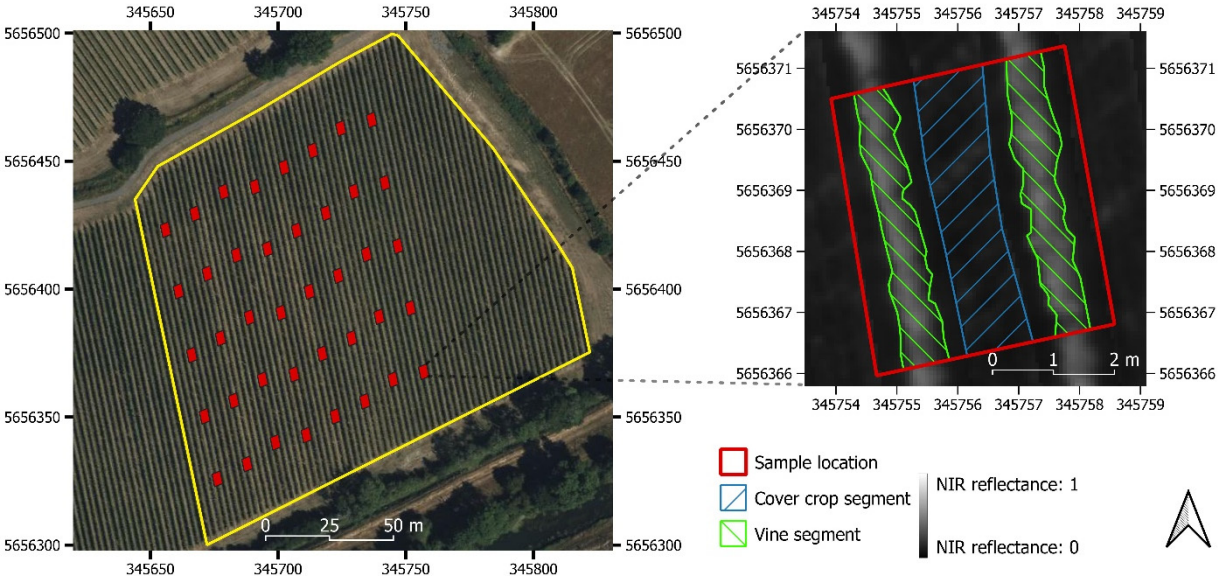

Figure 2. (**Left**): an example of a sampling strategy at Bottom Camp, (**Right**): example of vine and cover-crop segmentation at the individual block of ten vines.

2.2. Remote Sensing Data Collection

2.2.1. UAV Image Acquisition

A total of nine flights were conducted to cover three harvest seasons across the three vineyards. For each instance, imagery was collected approximately two weeks prior to commercial harvest. UAV imagery was acquired using a Parrot Sequoia four-band multispectral sensor (Parrot, Paris, France). The Parrot Sequoia is an advanced complementary metal-oxide-semiconductor [10] sensor which captures spectral data in the green (550 + −40 nm), red (660 + −40), red edge (735 + −10 nm), and NIR (790 + −40) bandwidths [11]. It is principally designed to target vegetation features [12,13] and is frequently used within agricultural surveys [14]. Along with an integrated Global Positioning System (GPS) and inertial measurement unit (IMU), the Sequoia houses a downwelling sunshine sensor which automatically calibrates outputs to an absolute reflectance value [11]. Corrected reflectance values are vital for the comparison of temporally unique images due to inevitable variation in illumination levels. The sensor was mounted upon a DJI Matrice 600P UAV flying at a height of 50 m above the ground level with 10 m line spacing. Imagery was acquired every two seconds under a flight speed of 3–4 m/s, resulting in a >80% image overlap. For each yearly data collection, the three sample fields were captured within a four-hour window between 10 a.m. and 2 p.m., to ensure consistently high levels of incident radiation and minimal shadows cast by vines. Over the entire field campaign, a downwelling sensor onboard the Parrot Sequoia was used to correct the radiance values to reflectance values. The sensor was calibrated at the start of each data collection.

2.2.2. Sentinel-2 Data Download

A Sentinel-2 image was downloaded from the 1–2-week period prior to harvest for each of the three survey years (image acquisition dates: 14 September 2020, 18 September 2021, 10 September 2022) from the Copernicus Open Access hub. Data were downloaded in Level 2a bottom-of-atmosphere reflectance and converted from the delivered format (reflectance × 10,000) to the 0–1 reflectance range.

2.3. Image Processing and Analysis

After screening for image quality, between 350 and 500 images were processed at each of the three sites using Pix4D v4.8.1 [15]. Mosaicking was undertaken to produce an orthomosaic for each bandwidth. Processing settings included a minimum of three match points, with Gaussian average downsampling with camera and sun irradiance corrections. The four orthomosaics per data collection were then further inspected in ArcGIS 10.8.1 to ensure geospatial accuracy. Orthomosaics were then masked to the boundary of each vineyard before vegetation indices (VIs) (Table 1) were calculated. Vine and cover-crop polygons (as shown in Figure 2) were manually created, ensuring they only selected pure pixels. Spectral data were then averaged within these polygons to produce a mean spectral value for both vine ($vine_{uav}$) and cover crop ($cover\text{-}crop_{uav}$) for each spectral parameter at the 165 sample locations. The distinct horizontal separation of vine and cover crop allowed for the successful and accurate segmentation of the two features.

Table 1. Spectral parameters for XGBoost models.

VI	Formula/Bandwidth	
	Sequoia	Sentinel-2a
Red	660 nm + −40 nm	664.6 + −15.5 nm
Green	550 nm + −40 nm	559.8 + −18 nm
NIR	790 nm + −40 nm	832.8 + −53 nm

Table 1. *Cont.*

VI	Formula/Bandwidth
NDVI	$\frac{\text{NIR} - \text{Red}}{\text{NIR} + \text{Red}}$
GNDVI	$\frac{\text{NIR} - \text{Green}}{\text{NIR} + \text{Green}}$
EVI2	$2.5 * \frac{\text{NIR} - \text{Red}}{\text{NIR} + 2.4 * \text{Red} + 1}$

Table 1 details the three ratio VIs calculated (NDVI, GNDVI, EVI2) alongside four single bandwidths (red, green, NIR). These VIs are highly popular within remote sensing literature and were applied in this study due to their association with plant biophysical characteristics (e.g., greenness and leaf area, photosynthetic activity, chlorophyll), which are reported to affect grape yield and quality [16,17]. They are also chosen due to their robustness to background interference from soil [18]. The six spectral parameters from vine_{uav}, $\text{cover-crop}_{\text{uav}}$, and Sentinel-2 were set as independent variables for extreme gradient boosting (XGBoost) modelling, with grape quality parameters as the dependent variables. XGBoost is a highly popular machine learning (ML) approach which is renowned for its robustness and avoidance of overfitting [19]. Among the 165 samples, 109 samples were used for training and 56 were used for model evaluation. Model building was performed using Scikit-Learn CVGridSearch [20], which automates hyperparameter tuning. To improve the model performance and avoid overfitting to training data, the hyperparameters detailed in Table 2 were assessed for each model. Model performance was assessed using the coefficient of determination (R^2), mean average error (MAE), and mean-squared error (MSE). The three evaluation metrics are calculated using the SciKit-learn Python package with y representing dependent variables and x representing the independent variables.

Table 2. XGBoost hyperparameter tuning using CVSearch.

Number of estimators	1000	1500	2000
Minimum child weight	0.5	1	3
Max depth	6	8	10
Learning rate	0.2	0.5	1
Subsampling column ratio	0.3	0.5	0.8

Further analysis for the similarity between UAV and Sentinel-2 was undertaken using the structural similarity index (SSIM) proposed by Wang et al. [21]. Defined by Equation (1), where x and y represent the two images, μ_x, μ_y represent the mean grey intensity, σ_x, σ_y represent the standard deviation of grey intensity, σ_{xy} represents the covariance of grey intensity, and C_1, and C_2 are constants. The SSIM assesses the similarity of image luminance, contrast, and structure within a kernel. With identical images scoring 1 and no similarity scoring 0.

$$SSIM(x,y) = \frac{(\mu_{x2} + \mu_{y2} + C_1)(\sigma_{x2} + \sigma_{y2} + C_2)}{(2\mu_x\mu_y + C_1)(2\sigma_{xy} + C_2)} \quad (1)$$

For application within this work, UAV NIR reflectance data were aggregated to 10 m × 10 m pixels to ensure that image dimensions match Sentinel-2 NIR data. The NIR band was selected for this analysis due to its larger spectral range. SSIM was then applied using the SciKit-image library using a 3 × 3 pixel kernel size [22].

2.4. Grape Quality Assessment

At each sample location, ten grapes were collected per vine to create a 100-grape sample per trellis block. Grape bunches were located by eye, ensuring that observation was with the purpose of ensuring that bunches are representative of the vineyard and absent of

disease. Ten bunches were then located and ten grapes blindly selected to minimise bias in selection. Grapes were picked from the top, bottom, vine-facing side, and inter-row facing side of the bunch to control for sunlight exposure and ripening potential variation within the bunch. The 100-grape samples were subject to laboratory processing within 24 h of picking to minimise the effect of decomposition. Samples were crushed and filtered before being centrifuged to separate the must and ensure particle size < 10 µm for refractometry. A 6 ml sample was placed on an OenoFoss Fourier Transform Infrared sensor to perform a scan of the sample through a full-mid infrared spectrum [23] with four output parameters, and then recorded for training machine learning models.

Analysis focused on the grape total acid measuring total hydrogen ions in the sample, which impacts the mouthfeel and taste of the wine [24]. TSS, measured in Brix, quantifies the sugar content of the sample, an important component for fermentation and alcohol content [25]. Also, alpha amino acids are a source of nitrogen for the fermentation process [26], and finally, the berry weight was measured as the weight of the 100 grape samples. Each of these quantifiable parameters are important for the final wine characteristics and are popular metrics within viticultural literature [27–32].

3. Results

3.1. Sentinel-2 and UAV Imagery

Figure 3 presents the reflectance values for NIR, red, and green bandwidths for UAV and Sentinel-2. Due to their operational altitudes and sensor parameters, the two platforms can acquire data at different spatial resolutions, UAV orthomosaics are presented at 0.063 m spatial resolution, and S2 orthomosaics are presented at 10 m spatial resolution. UAV and Sentinel-2 bandwidths are displayed as a reflectance value between 0 and 1 and highlight the interaction of the electromagnetic spectrum with vegetation and soil. Higher biomass vines will reflect more energy in the NIR wavelengths and absorb more energy in the red wavelengths, whilst lower biomass inter-row areas will have lower reflective and absorption behaviours. Due to this behaviour, the vine rows can be clearly observed in the higher-resolution UAV imagery. However, within the Sentinel-2 data, the spatial resolution being greater than the interrow space size (approximately 2.0 m) results in mixed-feature pixels where the vine cannot be separated from the cover crop.

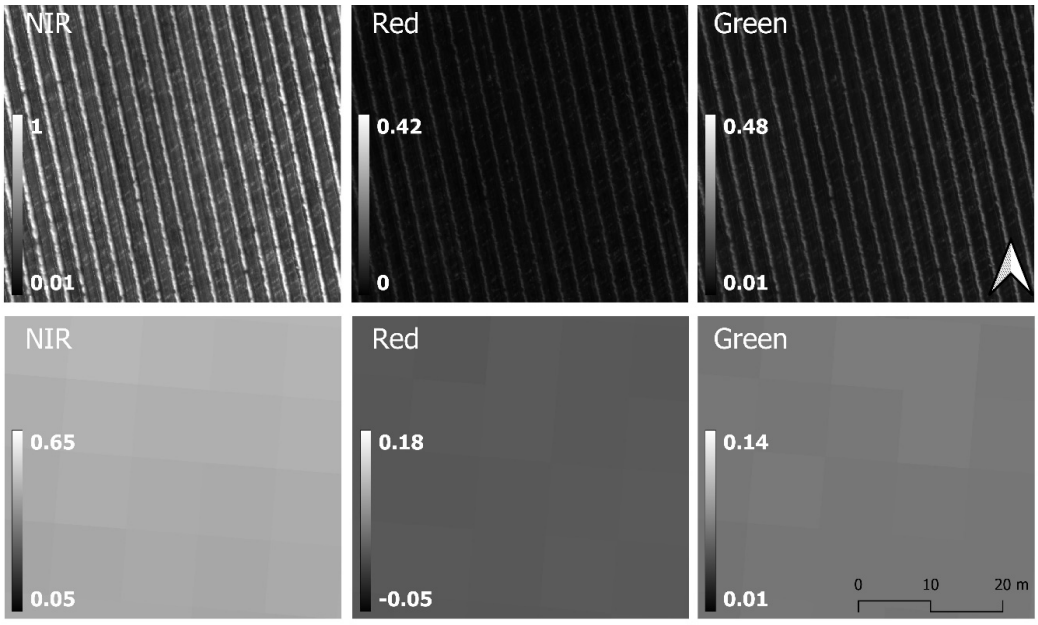

Figure 3. Near-infrared (NIR), red, and green bandwidths from UAV (**top**) and Sentinel-2 (**bottom**) were used in this study. The different resolutions between the platforms is evident, with the vine rows indiscernible within Sentinel-2 imagery.

3.2. Airborne Remote Sensing for Identifying Grape Yield and Quality Variation

Remote sensing UAV and Sentinel-2 data were input as independent variables within ML models to predict four grape yield and quality parameters. Model evaluation results for mixed-pixel Sentinel-2 data, pure $vine_{uav}$, and pure $cover\text{-}crop_{uav}$ pixels are presented in Tables 3–5 and Figures 4–6. These results are presented with the objective to understand the success of each sensor (UAV vs. Sentinel-2) and the spectral target (vine vs. cover crop) for predicting the grape yield and quality parameters.

Table 3 and Figure 4a–d present the model evaluation results and regression outputs for total acid, berry weight, alpha amino acid, and total soluble solids (Brix) from Sentinel-2 bands. The plots indicate the relationship between the remote sensing prediction and lab-derived yield and quality parameters. Total acid presents strong modelling results (R^2 = 0.60, MAE = 0.81 mg/L), TSS also demonstrates successful modelling but with a number of outliers where Sentinel-2 has over-predicted TSS values. Both total acid and TSS also present two clusters within the data. Alpha amino acid (Alpha) (R^2 = 0.44, MAE = 10.02 mg/L) and berry weight (R^2 = 0.18, MAE = 9.18 g) produce successful but weaker modelling results, with higher variance within predictions.

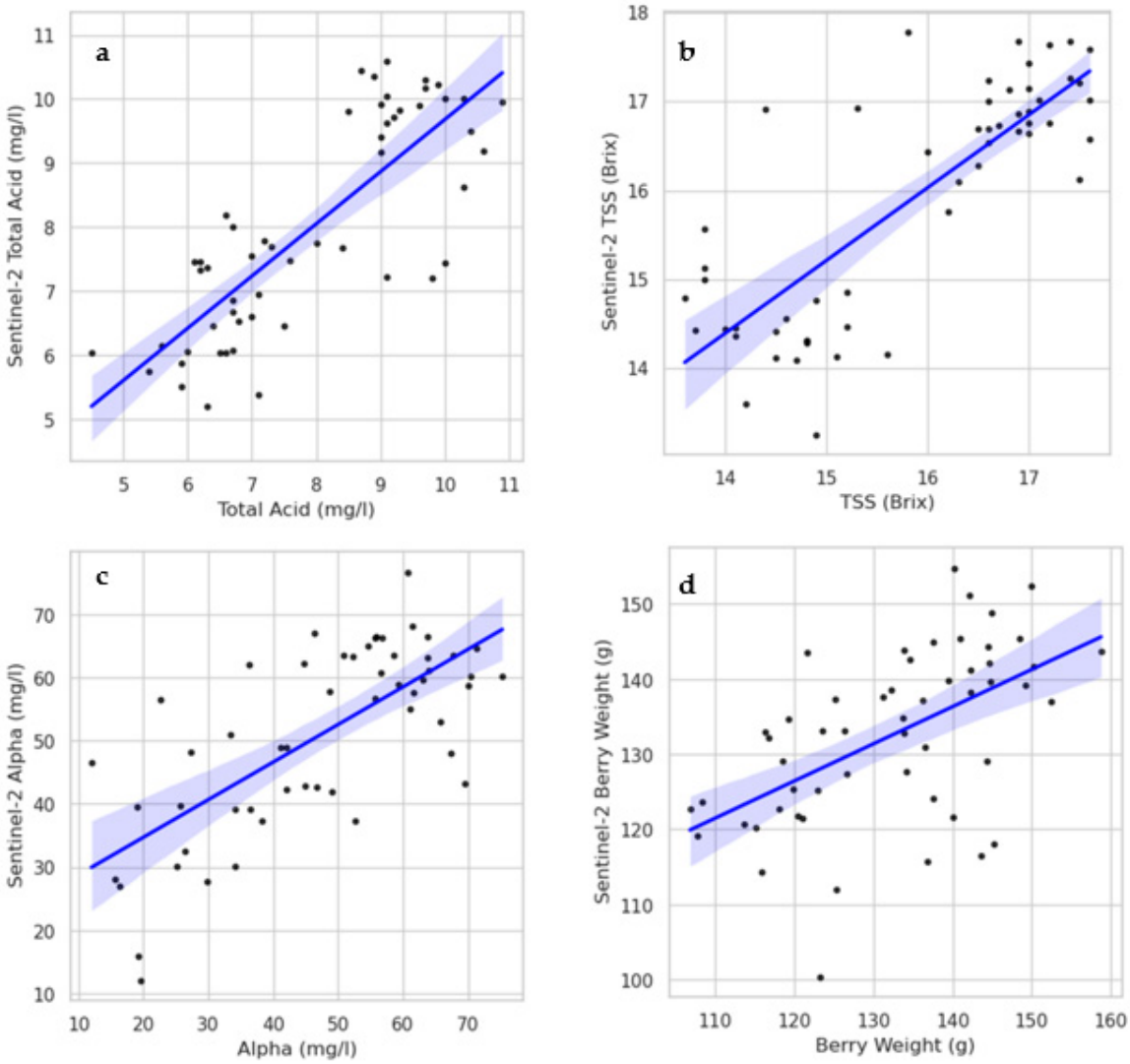

Figure 4. Sentinel-2 XGBoost regression outputs for four-grape yield and quality parameters (**a**): total acid; (**b**): total soluble solids; (**c**): alpha amino acids; and (**d**): berry weight. Results plot the predicted *Y* variable from remote sensing data against the observed laboratory-derived quality parameter. Shown with 95% confidence intervals.

Table 3. Extreme gradient boosting (XGBoost) model performance for the Sentinel-2 prediction of four yield and quality parameters. Model evaluation statistics include coefficient of determination (R^2), mean average error (MAE), and mean square error (MSE). Total acid range = 4.6 mg/L, alpha amino acid range = 71.8 mg/L, total soluble solids (TSSs) range = 5.5 Brix, berry weight range = 53.3 g.

	Total Acid (mg/L)	Alpha (mg/L)	TSS (Brix)	Berry Weight (g)
R^2	0.60	0.44	0.60	0.18
MAE	0.81	10.02	0.59	9.18
MSE	1.02	12.85	0.81	11.51

Table 4 and Figure 5a–d present the model evaluation results and regression outputs from $vine_{uav}$ bandwidths and VIs. The results demonstrate the successful modelling of total acid (R^2 = 0.67, MAE = 0.73 mg/L) and TSS (R^2 = 0.77, MAE = 0.50 Brix), yet consistent with Sentinel-2 results, clear clusters of values are again present. Alpha amino acid (R^2 = 0.58, MAE = 8.29) and berry weight (R^2 = 0.34, MAE = 8.22 g) are weaker models, with more variation; however, no clustering is observed.

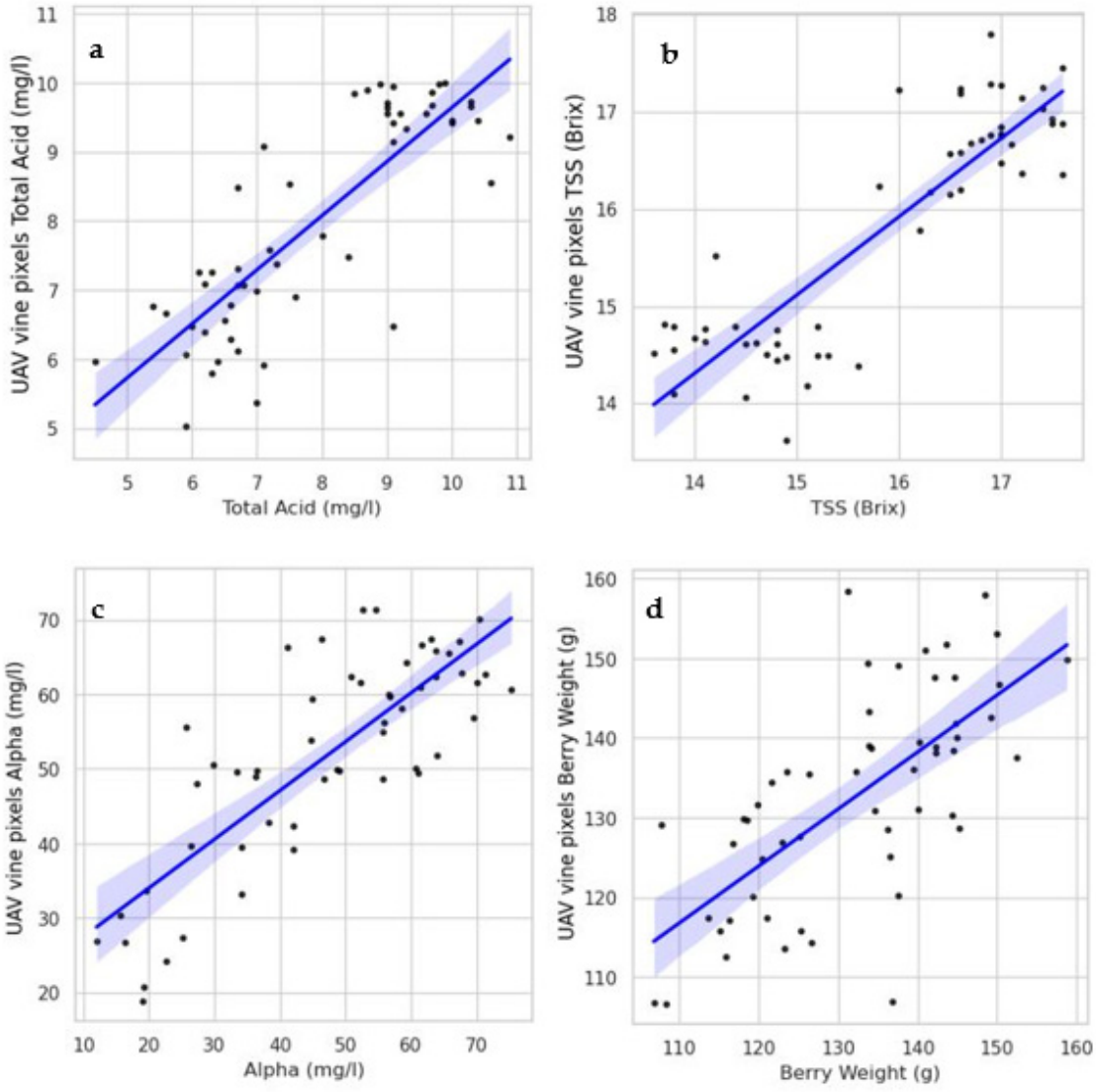

Figure 5. UAV vine XGBoost regression outputs for four grape yield and quality parameters ((**a**): total acid, (**b**): total soluble solids, (**c**): alpha amino acids, and (**d**): berry weight). Results plot the predicted *Y* variable from remote sensing data against the observed laboratory-derived quality parameter. Shown with 95% confidence intervals.

Table 4. Extreme gradient boosting (XGBoost) model performance for the pure vine$_{uav}$ pixels prediction of four yield and quality parameters. Model evaluation statistics include a coefficient of determination (R^2), mean average error (MAE), and mean square error (MSE). Total acid range = 4.6 mg/L, alpha amino acid range = 71.8 mg/L, total soluble solids (TSSs) range = 5.5 Brix, berry weight range = 53.3 g.

	Total Acid (mg/L)	Alpha (mg/L)	TSS (Brix)	Berry Weight (g)
R^2	0.67	0.58	0.58	0.32
MAE	0.73	8.29	0.50	8.22
RMSE	0.93	11.09	0.68	10.35

Table 5 and Figure 6a–d present the model evaluation results and regression outputs from cover-crop$_{uav}$ bandwidths and VIs. The results demonstrate the successful modelling of total acid (R^2 = 0.45, MAE = 0.93 mg/L) and TSS (R^2 = 0.45, MAE = 0.76 Brix); yet, consistently with Sentinel-2 results, the clear clusters of values are again present. Alpha amino acid (R^2 = 0.43, MAE = 10.02) and berry weight (R^2 = 0.37, MAE = 8.10 g) produce similar model performance metrics with a limited evidence of clustered values.

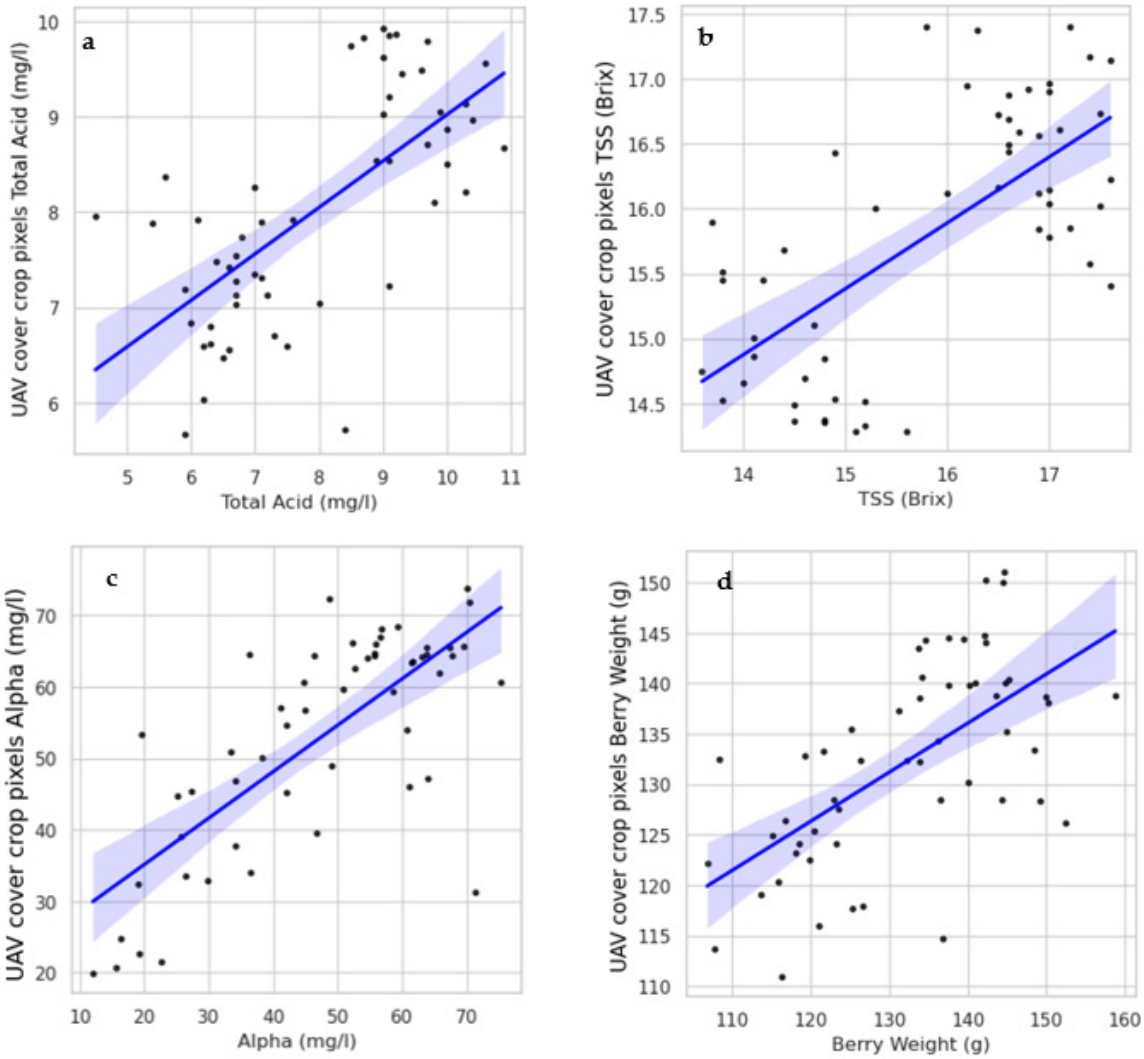

Figure 6. UAV-derived cover-crop XGBoost regression outputs for four grape yield and quality parameters ((**a**): total acid, (**b**): total soluble solids, (**c**): alpha amino acids, and (**d**): berry weight). Results plot the predicted *Y* variable from remote sensing data against the observed laboratory-derived quality parameter. Shown with 95% confidence intervals.

Table 5. Extreme gradient boosting (XGBoost) model performance for pure cover-crop$_{uav}$ pixels' prediction of four yield and quality parameters. Model evaluation statistics include the coefficient of determination (R2), mean average error (MAE), and mean square error (MSE). Total acid range = 4.6 mg/L, alpha amino acid range = 71.8 mg/L, total soluble solids (TSSs) range = 5.5 Brix, berry weight range = 53.3 g.

	Total Acid (mg/L)	Alpha (mg/L)	TSS (Brix)	Berry Weight (g)
R^2	0.45	0.43	0.45	0.37
MAE	0.93	10.02	0.76	8.10
RMSE	1.21	13.00	0.95	10.09

R^2 values between UAV and Sentinel-2 platforms and the vine$_{uav}$ and cover-crop$_{uav}$ suggest that modelling is successful; however, prediction strength is limited. Sentinel-2 models for total acid, TSS, and alpha amino acid produce similar model success to vine$_{uav}$ models, whilst berry weight predictions were weak for each methodology. Pure cover-crop$_{uav}$ produced successful models; however, R^2 values ranging between 0.37 and 0.45 were marginally weaker than both pure vine$_{uav}$ and Sentinel-2 models.

3.3. The Spectral Similarity Between UAV and Sentinel-2 Acquired Data

With model evaluation results evidencing that remote sensing data from both UAV and Sentinel-2 can successfully predict grape yield and quality parameters, the following results will compare the similarity between UAV and Sentinel-2 imagery. Within viticultural literature, the authors stated the inhibiting influence of the inter-row space and cover crop upon Sentinel-2 imagery when attempting to monitor vine variation. Quantifying the similarity of the two platforms will aid in understanding of the influence vine and cover-crop spectra upon a mixed-feature Sentinel-2 image.

Figures 7–9 present Sentinel-2 10 m NIR and 10 m resampled UAV data, alongside the difference raster and SSIM outputs for three vineyards in 2022. Firstly, across the three vineyards, the maximum difference in NIR reflectance is between 0.15 and 0.20, with one pixel falling above 0.20, suggesting that despite a difference in observation dates, NIR reflectance is highly similar between the two platforms. BC is the least similar vineyard, with areas to the north and east with multiple pixels of NIR difference above 0.15. An edge effect can also be observed in BC and BH, where NIR values drop significantly around the edge of the image due to bare ground areas in the vineyard headland.

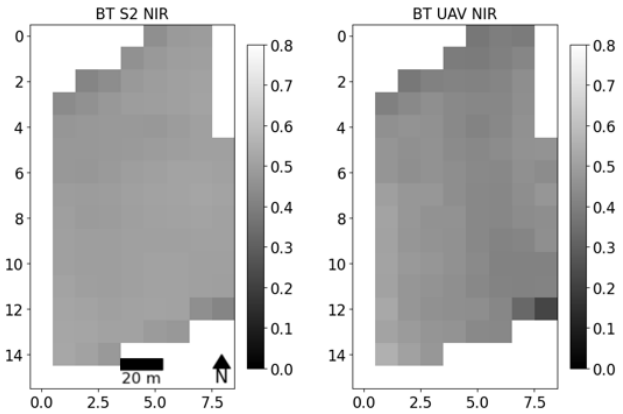

Figure 7. *Cont.*

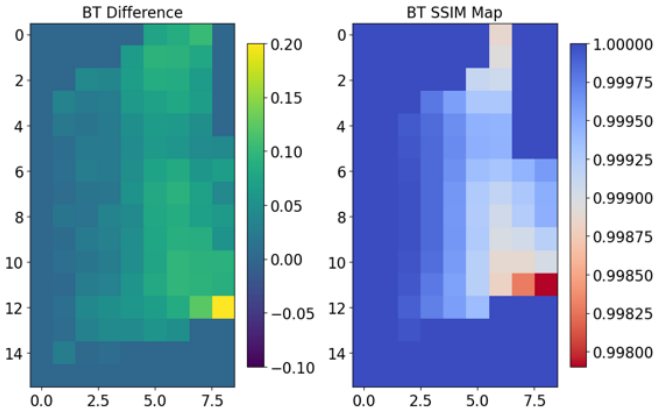

Figure 7. Structure similarity index and difference between Sentinel-2 (S2) near-infrared (NIR) and uncrewed aerial vehicle (UAV) NIR data at Butness (BT).

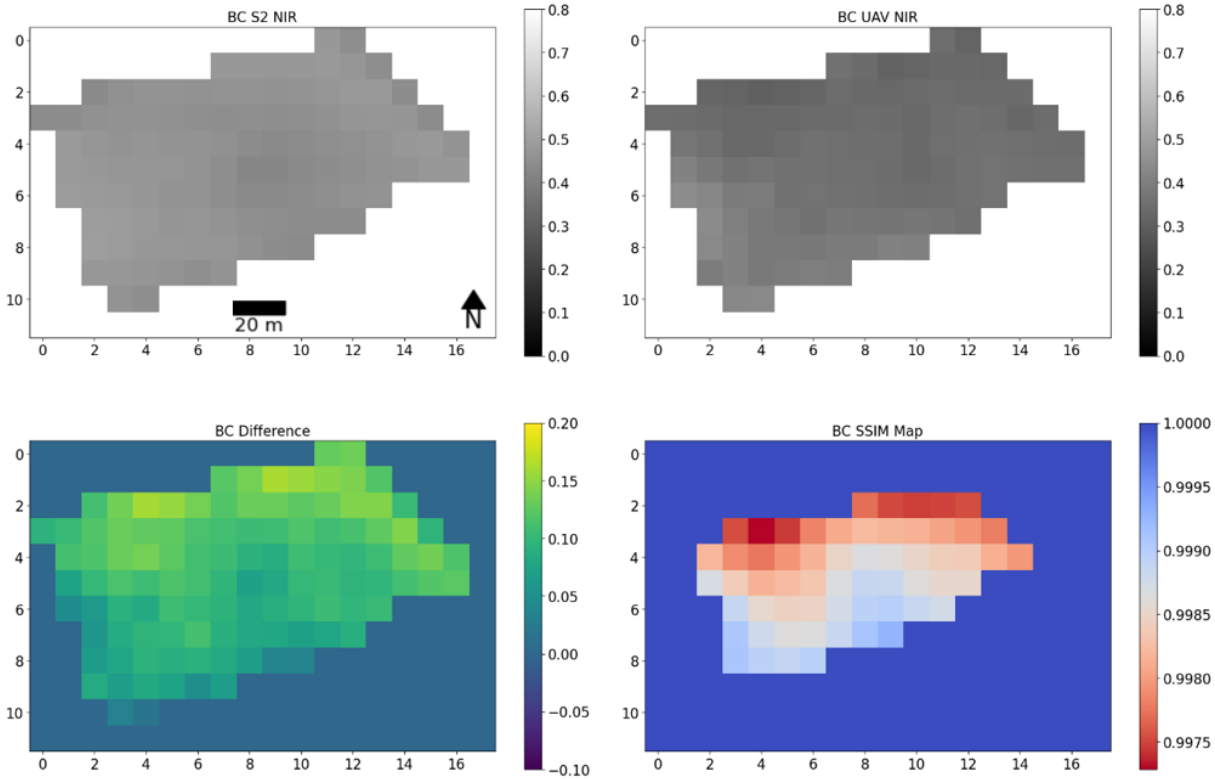

Figure 8. Structure similarity index and difference between Sentinel-2 (S2) near-infrared (NIR) and unmanned aircraft vehicle (UAV) NIR data at Bottom Camp (BC).

SSIM quantifies the similarity of images based on their luminance, contrast, and structure, with values of 1 representing identical images and values of 0 representing images with no similarity. To note, the SSIM raster does not report the edge pixels where a 3×3 kernel cannot be applied. The SSIM for all three vineyards is very high, with overall SSIM scores in excess of 0.99. Using a 3×3 pixel kernel, the SSIM score suggests that the Sentinel-2 and UAV rasters have similar pixel values and spatial structures. Across the three rasters, the least similar pixels are located in areas where the NIR difference value is highest. In BC, these pixels are found to the north and east of the image, whilst for BT, the lower SSIM score is observed near a single pixel which has a large NIR difference between the two platforms. A further observation is the apparent gradient of SSIM, occurring from left to right in BT and BH, and then from bottom to top in BC.

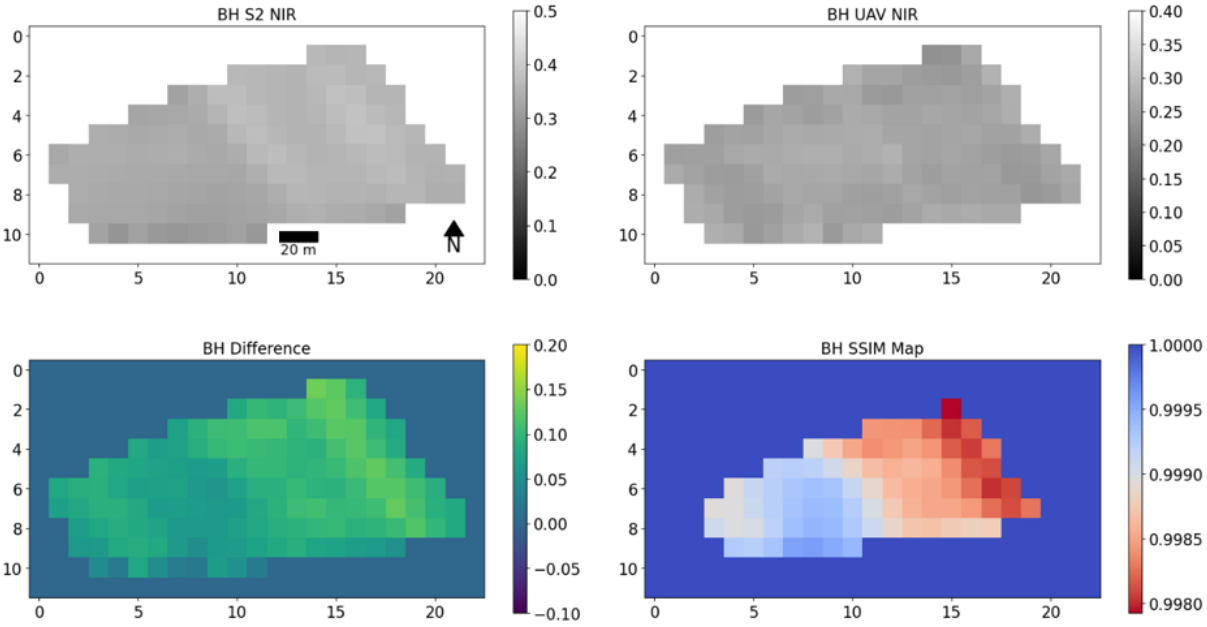

Figure 9. Structure similarity index and difference between Sentinel-2 (S2) near-infrared (NIR) and uncrewed aerial vehicle (UAV) NIR data at Boothill (BH).

SSIM has identified that the spatial similarity between UAV NIR and Sentinel-2 NIR is exceptionally high. To understand the individual effects of cover-crop and vine spectra upon Sentinel-2 imagery, the $vine_{uav}$ and $cover\text{-}crop_{uav}$ values are plotted against their spatially corresponding Sentinel-2 pixel in Figure 10. Across the three sample vineyards, it is clear that $cover\text{-}crop_{uav}$ NDVI (R = 0.954) holds a more linear relationship with Sentinel-2 NDVI than $vine_{uav}$ NDVI (R = 0.547). The data values are largely clustered by both the sample year and sample vineyard, with BT $cover\text{-}crop_{uav}$ reporting the highest NDVI values (NDVI = 0.88–0.92) for both UAV and Sentinel-2 imagery. BC and BH present a 0.20 NDVI difference between the sample years, whilst BT presents as a single larger cluster for both $vine_{uav}$ and $cover\text{-}crop_{uav}$ NDVI. Whilst it is clear that considering results by individual sample vineyard and sample year reduces the strength of the relationship, this intra-vineyard relationship is still significant on six occasions for $cover\text{-}crop_{uav}$ and on no occasion for $vine_{uav}$.

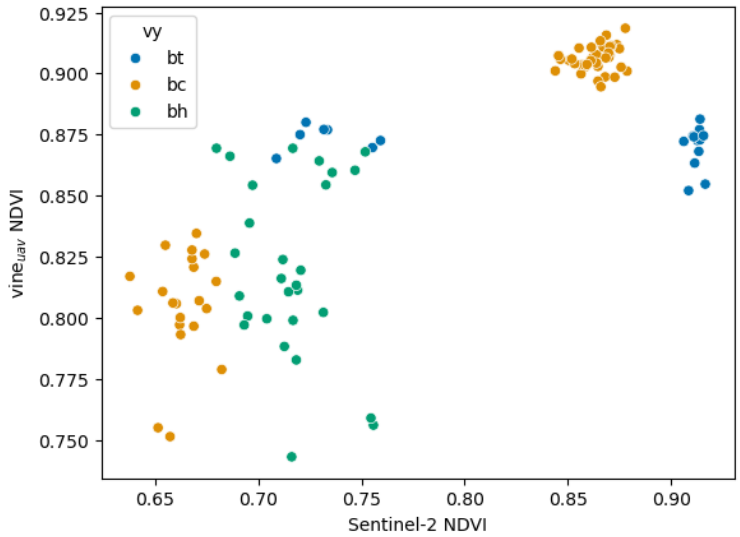

(**a**)

Figure 10. *Cont.*

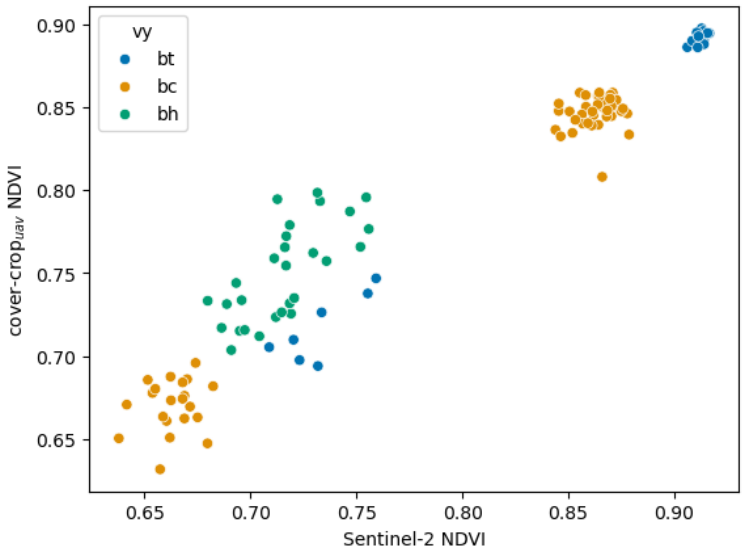

(**b**)

Figure 10. The relationship between S2 NDVI with vine$_{uav}$ NDVI (**a**) and cover-crop$_{uav}$ NDVI (**b**) with data points classified by sample vineyard: Bottom Camp (bc), Boothill (bh), and Butness (bt).

4. Discussion

4.1. Grape Quality Modelling Using Cover Crops and Machine Learning

This research assessed the ability of drone-derived vine and cover-crop pixels and mixed-feature Sentinel-2 pixels to predict grape yield and quality parameters. With the segmentation of high-resolution UAV imagery, further understanding was gained on the roles that cover-crop spectra play in the application of medium-resolution satellite imagery for vineyard monitoring.

The presented results show successful models across the three sets of spectral data (Sentinel-2, vine$_{uav}$, cover-crop$_{uav}$) and the four quality parameters (total acid, TSS, alpha amino acid, and berry weight). These outputs support the use of remote sensing data and machine learning models to predict multiple important and industry-recognised wine quality parameters which have a significant bearing on the flavour and mouthfeel of the wine [24,32], whilst further understanding the spatial variability of grape yield and quality can improve vineyard management and allow selective harvesting [6]. Therefore, the accurate monitoring of these parameters is essential for the business success of a vineyard.

Among these successful models, perhaps the most significant finding from this research is the outputs of cover-crop$_{uav}$ models. This is the first research to evidence that cover-crop spectra, acquired from high-resolution data, can be utilised within machine learning modelling to predict grape yield and quality parameters. For the total acid, TSS, and alpha amino acid, vine models only marginally outperformed cover-crop$_{uav}$ models (R^2 difference: total acid = −0.22, TSS = −0.23, alpha amino acid = −0.25), whilst for berry weight, the cover-crop$_{uav}$ produced a stronger model evaluation than vine$_{uav}$ models (R^2 difference: berry weight = +0.05). The comparability of these models suggests a relationship between cover-crop spectra and grape quality parameters. Within viticulture, growers will often use cover crop to help manage water availability and improve soil quality, therefore carefully controlling the vines' access to resources [33,34]. Evidence also exists that demonstrates plant-level interactions between cover crops and vines, with some authors further suggesting that these interactions also manifest within grape quality [35,36]. It is therefore possible that this interaction between cover crops and vines could be a mechanism through which cover-crop spectral variation can be linked to yield and quality. Whilst the results of this study are promising, viticultural literature remains inconclusive on the direct effect that cover crop has upon yield and quality. Despite the evidence presented by Bokulich et al. [37] and Chou et al. [35], comprehensive trial-based studies assessing different cover-

crop mixtures also found no direct effects upon grape quality parameters [36,38–40]. A second and more probable mechanism which may explain successful model results is an indirect relationship, where vines, cover crops, and grape yield and quality present parallel changes in their response to environmental changes (e.g., soil moisture and organic matter). Whilst this would be a proxy measurement of yield and quality, rather than measuring the direct effect of cover crop, this is the first study to evidence that cover crops have useful spectral data for grape yield and quality monitoring.

4.2. The Influence of Cover-Crop Spectra within Sentinel-2 Imagery

A second important outcome of this study which builds upon findings that cover-crop spectra hold beneficial information for monitoring is the effect that cover crop has upon mixed-feature medium-resolution satellite imagery, such as Sentinel-2. Previous research has largely stated that cover-crop and inter-row spaces act as noise when monitoring the vineyard [3–6], therefore rationalising the use of high-resolution UAV imagery to ensure that pure vine pixels can be acquired for monitoring.

In this work, SSIM results (Figures 7–9) between 10 m resampled UAV and Sentinel-2 imagery suggest that the luminance, contract, and structure is highly similar (SSIM = > 0.99). Therefore, it can be stated with certainty that spectrally, both platforms have similar representations of vineyard variance, whilst spatial resolution (UAV = 0.063 m, Sentinel-2 = 10 m) remains the most significant difference. Further exploring this similarity and assessing the relationship of $vine_{uav}$ and $cover\text{-}crop_{uav}$ NDVI to Sentinel-2 NDVI reveals that $cover\text{-}crop_{uav}$ holds a significantly more linear relationship (r-value = 0.954) to Sentinel-2 than $vine_{uav}$ (r-value = 0.547) across the three sample years and three sample vineyards. The strength of this result suggests that cover crop has a larger influence on a 10 m Sentinel-2 pixel than vine spectra. Therefore, in practice, the use of a moderate-resolution satellite to monitor a vineyard with similar presentation to that in this study will describe the spectral variance of the cover crop more than the spectral variance of the vines. This is likely the product of the cover crop having a larger spatial area than a vine within each 10 m pixel.

Conclusions reached by Matese et al. [4], Di Gennaro et al. [2], and Khaliq et al. [5], which aimed to monitor vine variation from moderate-resolution satellite imagery, state that the cover crop inhibits the ability to monitor vines. As shown in this study, cover-crop spectra have a higher influence on the Sentinel-2 pixel than the vine spectra, which will lead to the vine signal being obscured within a Sentinel-2 pixel. Therefore, a cover crop could be viewed as a hindrance when trying to monitor the vines.

Interestingly, within this study, the focus is not on assessing the vine in isolation, but instead, attempting to model yield and quality variation. This study has shown that these two parameters (yield and quality) are significantly correlated with the $cover\text{-}crop_{uav}$, and thus, a Sentinel-2 mixed pixel is capable of describing the variation in grape quality parameters due to both vine and cover-crop spectra being beneficial for modelling.

In summary, this study finds no evidence that cover-crop spectra inhibits the ability to monitor grape yield and quality and should be considered within future airborne remote sensing monitoring. With cover-crop spectra being viewed as useful, the value of moderate-resolution satellite imagery for monitoring grape yield and quality then increases. Despite operating at lower spatial resolutions than UAV imagery, open access sensors such as Sentinel-2 and Landsat-9 could provide yield and quality prediction models for very low material costs; and over larger spatial scales. As discussed by Matese et al. [4], compared to UAV which requires trained operators and equipment, monitoring vineyards over 50 ha is significantly more cost-effective using satellite imagery.

4.3. Limitations and Recommendations

Within viticultural remote sensing, there are many factors which complicate data acquisition and analysis, affecting the clarity of the results. Within this study, a prominent issue was the use of a multi-vineyard and multi-year strategy. This approach introduced significant variation within remote sensing data which likely had a bearing on machine

learning methodologies, clustering the data and likely inflating R^2 values. It is possible that the results represent the variance between sample years and sample vineyards more than the inter-vineyard variance. Whilst confidence remains in the ability of this methodology to identify inter-vineyard variation, future work would be more impactful, focusing on inter-field variation from a single survey. However, generating a yield and quality sample size large enough for training machine learning models remains a challenge due to the impact of sampling upon the commercial operations of the vineyard. Alternatively, exploring methodologies to normalise variance between sample years and vineyards could also be impactful research.

A second difficulty encountered throughout this work was the effect of vine shadows cast across the cover crop. This issue is discussed at length by Sozzi et al. [41], and despite targeting high-noon for data capture, shadows often persisted within UAV orthomosaics and could be exacerbating the spectral difference between vineyards. Whilst ratio normalisation VIs such as the NDVI largely mitigate the presence of shadows and variation in illumination levels across the scene, shadows likely remained a significant driver of difference in UAV surveys between the three vineyards. This impact of shadows could be minimised through selective UAV survey timings and sun position, but this is complex planning for large or commercial vineyards.

A prominent discussion within the literature also focuses on the timing of monitoring. Whilst UAV surveys in this study were completed one to two weeks prior to harvest, evidence suggests that targeting the veraison period (approximately 1 month prior to harvest) produces the strongest correlations with grape quality parameters [42]. Future works focusing on a multi-temporal monitoring design, collating the results of multiple remote sensing data collections per growing season, could lead to significant improvements in the modelling of grape yield and quality. Whilst also providing data to inform management decisions, this could allow for varied canopy management, selective harvesting, and improved harvest timing [43].

5. Conclusions

This paper investigated the ability of vine and cover-crop data acquired by high-resolution UAV and mixed-feature Sentinel-2 data to predict grape yield and quality parameters within an English vineyard. Successful modelling presents novel evidence of the link between cover-crop spectra and grape yield and quality data. Moreover, demonstrating the significance of cover-crop spectra then provides a mechanism through which Sentinel-2 mixed pixels can be used for yield- and quality-monitoring. This work has built on previous research which states the significant roles that inter-row space and cover crop play in viticultural remote sensing. Yet, it has also demonstrated that cover-crop spectra are not just noise and can be exploited to innovate remote sensing solutions within viticulture. Whilst moderate-resolution satellite imagery provides a very-low-cost monitoring solution, the importance of cover-crop spectra will also be vital for rapidly developing hyperspectral satellite solutions. Operating at a moderate resolution (8–30 m), the effect and possible value of cover-crop spectra will be increasingly prominent within future viticultural remote sensing.

Author Contributions: M.W. and N.G.B. undertook the fieldwork for the project. M.W., N.G.B., C.B.J. and M.B. developed the concepts and developed data analysis, and all authors reviewed the manuscript. All authors have read and agreed to the published version of the manuscript.

Funding: The funding provided by University of Brighton and NIAB.

Data Availability Statement: The data presented in this study are available on request from the corresponding author due to the sensitivity of data collection at a commercial vineyard.

Acknowledgments: We would like to thank the contributions of my supervisors, Niall Burnside, Matthew Brolly, and Chris Joyce throughout this study. Also, we are grateful for the external contributions of Julien Lecourt and Mark Else at the National Centre of Agricultural Botany (NIAB).

Conflicts of Interest: The authors declare no conflicts of interest.

References

1. Fernández-Novales, J.; Saiz-Rubio, V.; Barrio, I.; Rovira-Más, F.; Cuenca-Cuenca, A.; Santos Alves, F.; Valente, J.; Tardaguila, J.; Diago, M.P. Monitoring and mapping vineyard water status using non-invasive technologies by a ground robot. *Remote Sens.* **2021**, *13*, 1828. [CrossRef]
2. Di Gennaro, S.F.; Matese, A.; Gioli, B.; Toscano, P.; Zaldei, A.; Genesio, L. A low-cost and unsupervised image recognition methodology for yield estimation in a vineyard. *Front. Plant Sci.* **2019**, *10*, 559. [CrossRef] [PubMed]
3. Zarco-Tejada, P.J.; Berjón, A.; López-Lozano, R.; Miller, J.R.; Martín, P.; Cachorro, V.; González, M.R.; De Frutos, A. Assessing vineyard condition with hyperspectral indices: Leaf and canopy reflectance simulation in a row-structured discontinuous canopy. *Remote Sens. Environ.* **2005**, *99*, 271–287. [CrossRef]
4. Matese, A.; Di Gennaro, S.F.; Genova, G.; Orlandini, S.; Valentini, R. Intercomparison of UAV, aircraft, and satellite remote sensing platforms for precision viticulture. *Remote Sens.* **2015**, *7*, 2971–2990. [CrossRef]
5. Khaliq, A.; Comba, L.; Biglia, A.; Ricauda Aimonino, D.; Tortia, C.; Gay, P. Comparison of satellite and UAV-based multispectral imagery for vineyard variability assessment. *Remote Sens.* **2019**, *11*, 436. [CrossRef]
6. Kasimati, A.; Kotsopoulos, S.; Ntanos, S. Investigating a selection of methods for the prediction of total soluble solids among wine grape quality characteristics using normalized difference vegetation index data from proximal and remote sensing. *Front. Plant Sci.* **2021**, *12*, 627974. [CrossRef]
7. Caspari, H.; Neal, S.; Naylor, A. Cover crop management in vineyards to enhance deficit irrigation in a humid climate. *II Int. Symp. Irrig. Hortic. Crops* **1996**, *449*, 313–320. [CrossRef]
8. Afonso, J.; Monteiro, A.; Lopes, C.; Lourenço, J. Enrelvamento do solo em vinha na região dos vinhos verdes. Três anos de estudo na casta 'Alvarinho'. *Ciência Técnica Vitivinícola* **2003**, *18*, 47–63. Available online: https://www.passeidireto.com/arquivo/145793470/enrelvamento-do-solo-em-vinha-na-regiao-dos-vinhos-verdes-tres-anos-de-estudo-na (accessed on 25 October 2023).
9. Chan, K.Y.; Fahey, D.J.; Nandra, H.S. Using composted mulch in vineyards—Effects on grape yield and quality. *Int. J. Fruit Sci.* **2010**, *10*, 441–453. [CrossRef]
10. Weste, N.; Harris, D. *CMOS VLSI Design: A Circuits and Systems Perspective*, 3rd ed.; Pearson/Addison-Wesley: Boston, MA, USA, 2004.
11. Sensefly. Parrot Sequoia 2004, Multispectral Camera. Sensefly. 2022. Available online: https://www.parrot.com/uk/support/documentation/sequoia (accessed on 3 May 2022).
12. Franklin, S.E.; Ahmed, O.S.; Williams, G. Northern conifer forest species classification using multispectral data acquired from an unmanned aerial vehicle. *Photogramm. Eng. Remote Sens.* **2017**, *83*, 501–507. [CrossRef]
13. Franzini, M.; Dubbini, M.; Zani, D.; Gattelli, M. Geometric and radiometric consistency of Parrot Sequoia multispectral imagery for precision agriculture applications. *Appl. Sci.* **2019**, *9*, 5490. [CrossRef]
14. Negash, L.; Kim, H.-Y.; Choi, H.-L. Emerging UAV applications in agriculture. In Proceedings of the 2019 7th International Conference on Robot Intelligence Technology and Applications (RiTA), Daejeon, Republic of Korea, 1–3 November 2019; IEEE: Piscataway, NJ, USA, 2019; pp. 175–180. [CrossRef]
15. Pix4D. Pix4Dmapper User Manual (Revision 4.1); Pix4D. 2017. Available online: https://support.pix4d.com/hc/en-us/articles/205751415 (accessed on 25 October 2023).
16. Hardy, P.J. Metabolism of sugars and organic acids in immature grape berries. *Plant Physiol.* **1968**, *43*, 224–228. [CrossRef] [PubMed]
17. van Leeuwen, C.; Destrac Irvine, A. Modified grape composition under climate change conditions requires adaptations in the vineyard. *OENO One* **2017**, *51*, 147–154. [CrossRef]
18. Huete, A.R. A soil-adjusted vegetation index (SAVI). *Remote Sens. Environ.* **1988**, *25*, 295–309. [CrossRef]
19. Chen, T.; Guestrin, C. XGBoost: A scalable tree boosting system. In Proceedings of the 22nd ACM SIGKDD International Conference on Knowledge Discovery and Data Mining, San Francisco, CA, USA, 13–17 August 2016; Association for Computing Machinery: New York, NY, USA, 2016; pp. 785–794. [CrossRef]
20. Buitinck, L.; Louppe, G.; Blondel, M.; Pedregosa, F.; Mueller, A.; Grisel, O.; Niculae, V.; Prettenhofer, P.; Gramfort, A.; Grobler, J.; et al. API design for machine learning software: Experiences from the scikit-learn project. *arXiv* **2013**, arXiv:1309.0238.
21. Wang, Z.; Bovik, A.C.; Sheikh, H.R.; Simoncelli, E.P. Image quality assessment: From error visibility to structural similarity. *IEEE Trans. Image Process.* **2004**, *13*, 600–612. [CrossRef]
22. Scikit-Image (nd). SSIM. Structural Similarity Index—Skimage 0.24.0 Documentation. Available online: https://scikit-image.org/docs/stable/api/skimage.metrics.html#skimage.metrics.structural_similarity (accessed on 16 November 2023).
23. Foss. OenoFoss. Foss Analytics. 2022. Available online: https://www.fossanalytics.com/en/products/oenofoss (accessed on 22 January 2023).
24. Tsegay, Z.T. Total titratable acidity and organic acids of wines produced from cactus pear (*Opuntia-ficus-indica*) fruit and Lantana camara (*L. camara*) fruit blended fermentation process employed response surface optimization. *Food Sci. Nutr.* **2020**, *8*, 4449–4462. [CrossRef]
25. Urraca, R.; Sanz-García, A.; Tardaguila, J.; Diago, M.P. Estimation of total soluble solids in grape berries using a hand-held NIR spectrometer under field conditions. *J. Sci. Food Agric.* **2016**, *96*, 3007–3016. [CrossRef]

26. Fairbairn, S.; McKinnon, A.; Musarurwa, H.T.; Ferreira, A.C.; Bauer, F.F. The impact of single amino acids on growth and volatile aroma production by *Saccharomyces cerevisiae* strains. *Front. Microbiol.* **2017**, *8*, 2554. [CrossRef]
27. Usseglio-Tomasset, L. *Chimica Enologica*; HOEPLI: Milan, Italy, 1995.
28. Margalit, Y. *Concepts in Wine Chemistry (Rev. ed.)*; Ringgold Inc.: Bristol, UK, 2005.
29. Boulton, R.B.; Singleton, V.L.; Bisson, L.F.; Kunkee, R.E. *Principles and Practices of Winemaking*; Springer Science & Business Media: Berlin/Heidelberg, Germany, 2013.
30. Vilela, A. Use of nonconventional yeasts for modulating wine acidity. *Fermentation* **2019**, *5*, 27. [CrossRef]
31. Trimble, S. Brix as a Metric of Fruit Maturity. Felix Instruments. 2022. Available online: https://felixinstruments.com/blog/brix-as-a-metric-of-fruit-maturity/ (accessed on 5 April 2019).
32. Koone, R.; Harrington, R.J.; Gozzi, M.; McCarthy, M. The role of acidity, sweetness, tannin and consumer knowledge on wine and food match perceptions. *J. Wine Res.* **2014**, *25*, 158–174. [CrossRef]
33. Naylor, R.E.L.; Lutman, P.J.W. What is a weed. *Weed Res.* **2007**, *47*, 375–383. [CrossRef]
34. Pérez-Álvarez, E.; Garde-Cerdan, T.; Santamaría, P.; García-Escudero, E.; Peregrina, F. Influence of two different cover crops on soil N availability, N nutritional status and grape yeast assimilable N (YAN) in a Cv. Tempranillo vineyard. *Plant Soil* **2015**, *390*, 143–156. [CrossRef]
35. Chou, M.-Y.; van Heuvel, J.; Bell, T.H.; Panke-Buisse, K.; Kao-Kniffin, J. Vineyard under-vine floor management alters soil microbial composition, while the fruit microbiome shows no corresponding shifts. *Sci. Rep.* **2018**, *8*, 11039. [CrossRef]
36. Wheeler, S.J.; Black, A.; Pickering, G. Vineyard floor management improves wine quality in highly vigorous Vitis vinifera 'Cabernet Sauvignon' in New Zealand. *N. Z. J. Crop Hortic. Sci.* **2005**, *33*, 117–128. [CrossRef]
37. Bokulich, N.A.; Thorngate, J.H.; Richardson, P.M.; Mills, D.A. Microbial biogeography of wine grapes is conditioned by cultivar, vintage, and climate. *Proc. Natl. Acad. Sci. USA* **2014**, *111*, E139–E148. [CrossRef]
38. Trigo-Córdoba, E.; Bouzas-Cid, Y.; Orriols, I.; Diaz-Losada, E. Influence of cover crop treatments on the performance of a vineyard in a humid region. *Span. J. Agric. Res.* **2015**, *13*, e0907. [CrossRef]
39. Bouzas-Cid, Y.; Díaz-Losada, E.; Trigo-Córdoba, E.; Orriols, I. Effect of vegetal ground cover crops on wine anthocyanin content. *Sci. Hortic.* **2016**, *211*, 399–404. [CrossRef]
40. Pérez-Expósito, J.P.; Fernández-Caramés, T.M.; Fraga-Lamas, P.; Castedo, L. VineSens: An eco-smart decision-support viticulture system. *Sensors* **2017**, *17*, 465. [CrossRef]
41. Sozzi, M.; Kayad, A.; Marinello, F.; Taylor, J.; Tisseyre, B. Comparing vineyard imagery acquired from Sentinel-2 and unmanned aerial vehicle (UAV) platform. *OENO One* **2020**, *54*, 189–197. [CrossRef]
42. Lamb, D.W.; Bramley, R.G.V.; Hall, A. *Precision Viticulture—An Australian Perspective*; International Society for Horticultural Science (ISHS): Leuven, Belgium, 2004. [CrossRef]
43. Cunha, M.; Marçal, A.R.S.; Silva, L. Very early prediction of wine yield based on satellite data from VEGETATION. *Int. J. Remote Sens.* **2010**, *31*, 3125–3142. [CrossRef]